

Fluorescent Chemosensors Based on Energy Migration in Conjugated Polymers: The Molecular Wire Approach to Increased Sensitivity

Qin Zhou and Timothy M. Swager*

Contribution from the Department of Chemistry and Laboratory for Research on the Structure of Matter, University of Pennsylvania, Philadelphia, Pennsylvania 19104-6323

Received September 6, 1995[⊗]

Abstract: We demonstrate herein how conjugated polymers (molecular wires) can be used to interconnect (wire in series) receptors to produce fluorescent chemosensory systems with sensitivity enhancements over single receptor analogues. The enhancement mechanism in the polyreceptor materials is based on an energy migration scheme in which excitations, diffuse along the polymer backbone. Analyte binding produces trapping sites for the excitations which results in greatly attenuated emission intensity. Three different cyclophane-based receptor systems that bind paraquat were investigated. These systems are quenched by paraquat binding, and the quenching enhancements relative to a monomeric model compound were used to determine the efficiency of energy migration. Two polymers with related poly(phenyleneethynylene) structures were investigated, and the all-para system was found to exhibit more facile energy migration than the more electronically localized analogue that contained meta linkages. The para polyreceptor system was found to display a 65-fold enhancement in sensitivity to paraquat as compared to a model monoreceptor fluorescent chemosensor. However, we have determined that delocalization alone is not sufficient to produce facile energy migration, and the more delocalized polythiophenes appear to be less effective at energy migration than the para poly(phenyleneethynylene) material. Paraquat-induced fluorescent quenching studies on homologous polymers that lacked the cyclophane receptors were also performed. These results indicate that diffusive quenching by paraquat is enhanced by energy migration.

Introduction

The concept of a molecular wire became a reality nearly 20 years ago with the discovery of metallic conductivity in an organic polymer.¹ The ensuing advances in the understanding and synthesis of conjugated (conducting) polymers now allow for the design and synthesis of molecular wires with tailored properties.² There are many visionary applications of such materials in single-molecule photovoltaic devices³ and molecular electronics.⁴ We have been investigating molecule-based sensory materials in which synthetic receptors are connected directly to a conjugated polymer's backbone.⁵ Using this approach, we produce polyreceptor assemblies that are electronically connected or, in effect, "wired in series" by a conjugated polymer (molecular wire). We demonstrate herein that this approach to fluorescent chemosensors⁶ can present large sensitivity gains over more conventional molecule-based fluorescent chemosensors.

Attaining an enhanced chemosensory response using the molecular wire (polyreceptor) configuration requires that the

transduction event be a property of the collective system rather than a property determined by local electronic structure. For example, a property determined by local electronic structure is NMR chemical shift. Properties in conjugated polymers that are slightly less localized, but still not determined by a large collective system, are redox potential and optical absorption characteristics. On the other hand, conductivity is the quintessential example of a collective property in a conjugated (conducting) polymer, and the conductivity of conducting polymers has been long been understood to be limited by small amounts of defects. We recently demonstrated that conductivity is highly sensitive to minor perturbations resulting from analyte binding in receptor-containing polythiophenes.^{5b-d} In this report we show how energy migration, which is an additional transport property of conjugated polymers, can provide enhanced sensitivity in fluorescence-based chemosensors.

In the energy migration process, excitations that usually result from absorption of a photon migrate through the polymer (molecular wire). The precise mechanism of energy migration and the character of the excitations depend upon the system. Energy migration by Förster processes (dipole-dipole interactions) are well-known in nonconjugated polymers, and efficient antenna systems have been designed using this transport mechanism.⁷ Different mechanisms are operative in conjugated polymers, and these polymers appear to be very effective conduits for energy migration over long distances. For example, selective emission from states associated with anthracene end groups has been demonstrated in poly(phenyleneethynylenes), which indicates nearly quantitative energy transfer to the polymer's terminus.⁸ Energy migration is also thought to

[⊗] Abstract published in *Advance ACS Abstracts*, December 1, 1995.

(1) Chiang, C. K.; Fincher, C. R.; Park, Y. W.; Heeger, A. J.; Shirakawa, H.; Louis, E. J.; Gau, S. C.; MacDiarmid, A. G. *Phys. Rev. Lett.* **1977**, *39*, 1098.

(2) *Handbook of Conducting Polymers*; Skotheim, T. J., Ed.; Dekker: New York, 1986.

(3) Wrighton, M. S. *Comments Inorg. Chem.* **1985**, *4*, 269.

(4) (a) *Molecular Electronic Devices*; Carter, F. L., Ed.; Marcel Dekker: New York, 1982. (b) *Molecular Electronic Devices, II*; Carter, F. L., Ed.; Marcel Dekker: New York, 1987. (c) Hopfield, J. J.; Onuchic, J. N.; Beratan, D. N. *Science* **1988**, *241*, 817.

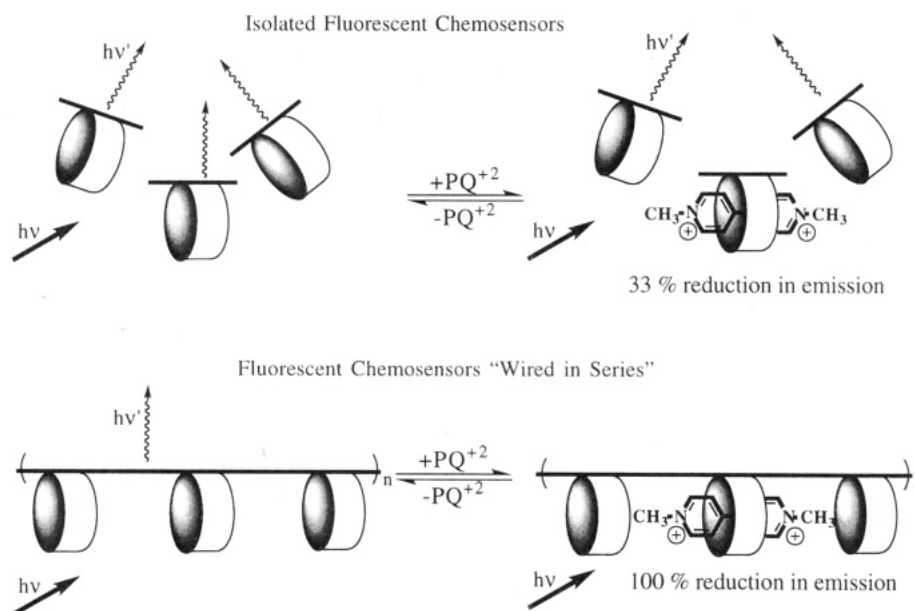
(5) (a) Marsella, M. J.; Swager, T. M. *J. Am. Chem. Soc.* **1993**, *115*, 12214. (b) Marsella, M. J.; Carroll, P. J.; Swager, T. M. *J. Am. Chem. Soc.* **1994**, *116*, 9347. (c) Marsella, M. J.; Carroll, P. J.; Swager, T. M. *J. Am. Chem. Soc.* **1995**, *117*, 9832. (d) Marsella, M. J.; Newland, R. J.; Carroll, P. J.; Swager, T. M. *J. Am. Chem. Soc.* **1995**, *117*, 9842.

(6) *Fluorescent Chemosensors for Ion and Molecular Recognition*; Czarnik, A. W., Ed.; ACS Symposium Series 538; American Chemical Society: Washington, DC, 1993.

(7) Guillet, J. *Polymer Photophysics and Photochemistry: An Introduction to the Study of Photoprocesses in Macromolecules*; Cambridge University Press: New York, 1987; Chapter 9.

(8) Swager, T. M.; Gil, C. J.; Wrighton, M. S. *J. Phys. Chem.* **1995**, *99*, 4886.

Scheme 1



influence the emission characteristics of electroluminescent devices based on conjugated polymers.⁹ Additionally, energy migration has been demonstrated in polysilanes, which have a delocalized σ band structure.¹⁰ Energy migration in conjugated polymers may occur by free carriers which move independently or by bound excitons.¹¹ Free carriers are favored by systems having a high electronic polarizability, which provides efficient screening of the electrostatic attractions and allows the excitations to dissociate into negative and positive carriers. It has been reported that the exciton binding energy is very low in poly(phenylenevinyls), and hence free carriers dominate.¹¹ In polydiacetylenes, which are less polarizable, the excitations behave as bound excitons.¹¹

We recently demonstrated an enhanced fluorescence chemosensory response using the molecular wire approach.¹² These studies made use of paraquat (PQ^{2+}), a well-known electron transfer quenching agent, as the analyte and cyclophane-based receptors, similar to those extensively investigated by Stoddart, as the recognition elements.¹³ These types of host-guest complexes are called pseudorotaxanes. The inherent sensitivity gain in such a polyreceptor ("wired in series") system over that of a discrete monoreceptor chemosensor can be understood from the schematic illustration in Scheme 1, wherein molecules are excited ($h\nu$) and emit ($h\nu'$). In a monoreceptor system with a high K_a , the fluorescence is quenched only in those receptor molecules forming pseudorotaxane complexes with PQ^{2+} , and the reduction in emission will be equal to the fractional occupancy of PQ^{2+} . In a molecular wire system, the excitation migrates throughout the polymer, sampling a multitude of receptor sites, and is quenched when it encounters a single pseudorotaxane site. Hence, in a polyreceptor system with fractional occupancies much less than shown in Scheme 1, all of the emission ($h\nu'$) will be quenched.

(9) Samuel, I. D. W.; Crystall, B.; Rumbles, G.; Burn, P. L.; Holmes, A. B.; Friend, R. H. *Chem. Phys. Lett.* **1993**, *213*, 472.

(10) (a) Wallraff, G. M.; Baier, M.; Diaz, A.; Miller, R. D. *J. Inorg. Organomet. Polym.* **1992**, *2*, 87. (b) Miller, R. D.; Baier, M.; Diaz, A. F.; Ginsburg, E. J.; Wallraff, G. M. *Pure Appl. Chem.* **1992**, *64*, 1291.

(11) Pakbaz, K.; Lee, C. H.; Heeger, A. J.; Hagler, T. W.; McBranch, D. *Synth. Met.* **1994**, *64*, 295.

(12) Zhou, Q.; Swager, T. M. *J. Am. Chem. Soc.* **1995**, *117*, 7017.

(13) (a) Allwood, B. L.; Spencer, N.; Shahriari-Zavareh, H.; Stoddart, J. F.; Williams, D. J. *J. Chem. Soc., Chem. Commun.* **1987**, 1064. (b) Amabilino, D. B.; Parsons, I. A.; Stoddart, J. F. *Trends Polym. Sci.* (Cambridge, UK) **1994**, *2*, 146 and references therein. (c) Anelli, P. L.; et al. *J. Am. Chem. Soc.* **1992**, *114*, 193.

For the process illustrated in Scheme 1, the maximum quenching enhancement of the molecular wire system over the isolated fluorescent chemosensors is a simple summation of the association constants for all the receptor units in the polymer. Hence, in the ideal case, wherein the association constants are additive and the diffusion length of the excitation exceeds the polymer's length, a maximum enhancement equal to the degree of polymerization will be obtained. If the diffusion length of the excitation is less than the polymer's length, due to low mobility and/or short lifetimes, the enhancement in the quenching effect will be somewhat less.

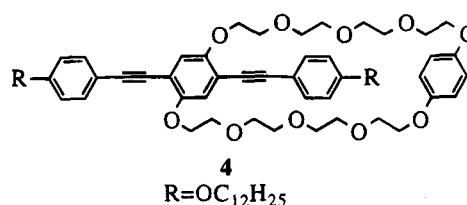
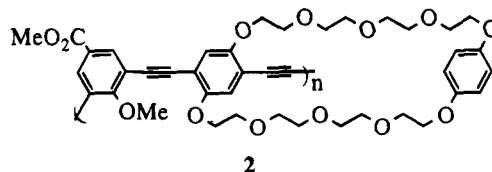
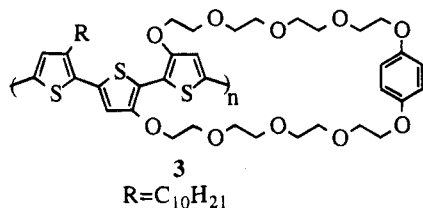
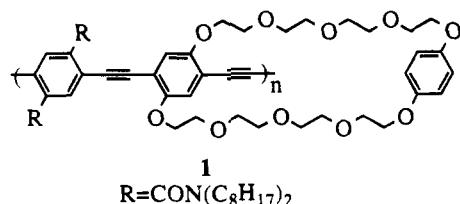
We have previously described greatly enhanced PQ^{2+} quenching in the cyclophane-containing polymer **1** relative to a low molar mass model compound **4** (Chart 1).¹² The degree of enhancement was shown to have a molecular weight dependence, first increasing at low M_n and then becoming insensitive to M_n above $\sim 65\,000$. This lack of increased sensitivity at high molecular weight indicates that the diffusion length of the excitation is less than the length of the polymer. For maximal sensitivity gains in single molecular wire based-fluorescent chemosensors, systems are required which display a combination of long-lived excitations states, excitations with high mobilities, and high molecular weights. As a first step toward understanding these interrelationships, we report herein detailed studies of **1** and investigations of two additional types of conjugated polymers that have different electronic structures. To probe delocalization in the poly(phenyleneethynylene) materials, we have synthesized polymer **2**. This polymer is closely related to **1** but has a significantly lower degree of delocalization as a result of its meta architecture. We also have studied polymer **3**, which is an example of a cyclophane-containing polymer that displays greater delocalization than **1**. This polymer has been previously shown to display a chemoresistive response with PQ^{2+} derivatives.^{5b,c}

Results and Discussion

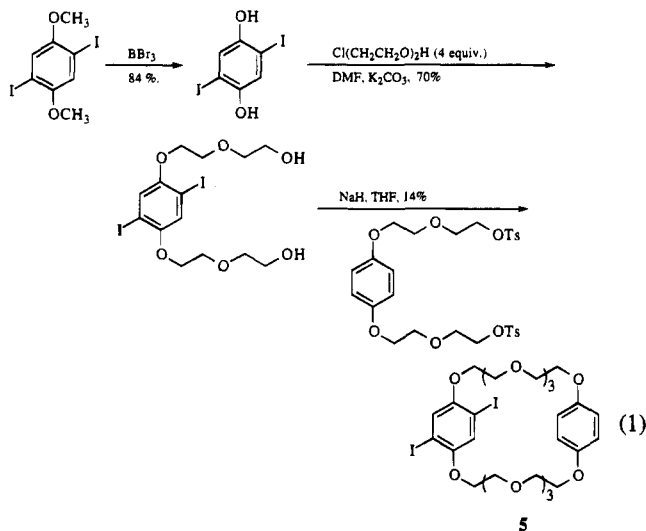
Synthesis. Palladium-catalyzed cross-coupling procedures were used extensively in the syntheses of all of the polymers, monomers, and other model compounds.¹⁴ These synthetic routes employ reactive organic halides both as monomers and

(14) Heck, R. F. *Palladium Reagents in Organic Syntheses*; Academic Press: Orlando, 1985.

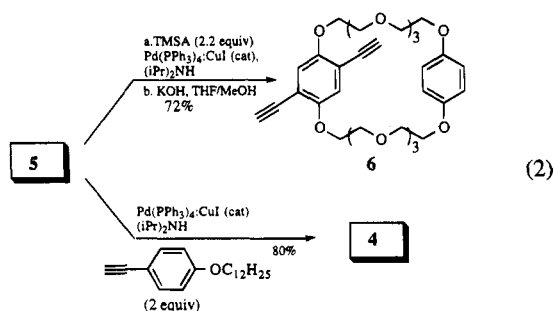
Chart 1



as intermediates in the synthesis of other monomers. Hence, the incorporation of cyclophane receptors into the polymers required the synthesis of iodinated derivatives (**5**) of a well-known paraquat receptor, bis(*p*-phenylene-34-crown-10).¹³ To produce this macrocycle, which is selectively iodinated on only one of the rings, we made use of a stepwise methodology similar to that previously reported.^{13c} As shown in eq 1, 1,4-diiodo-2,5-dihydroxybenzene is synthesized, appended with diethylene glycol groups, and then reacted with 1,4-bis[2-(2-hydroxyethoxy)ethoxy]benzene ditosylate and NaH to produce **5**.

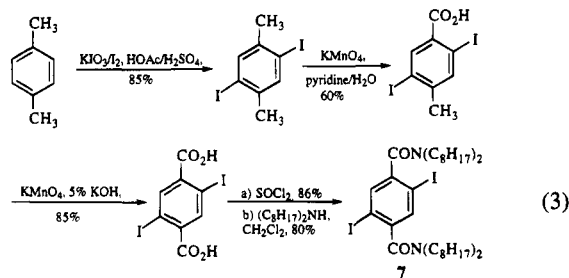


Compound **5** can be directly coupled with *p*-(dodecyloxy)-phenylacetylene to produce the model receptor **4** (eq 2). A similar coupling procedure with (trimethylsilyl)acetylene and subsequent desilylation produces monomer **6** (eq 2).

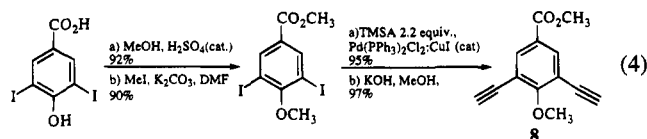


The efficient synthesis of monomer **7** required the oxidation of 2,6-diiodo-*p*-xylene by a two-step procedure (eq 3).¹⁵ Attempts to oxidize both of the methyl groups to carboxylic

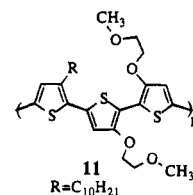
acids in one step gave unacceptably low yields.¹⁶ Alternatively, oxidation of 2,5-diiodo-*p*-xylene under mild basic conditions (6 equiv of KMnO₄, pyridine/H₂O) produces the monocarboxylate, which is readily isolated. The choice of pyridine as



solvent was important to maintain solubility throughout the reaction. The second oxidation step was then performed under strongly basic conditions with 4 equiv of KMnO₄ in KOH/H₂O to produce the dicarboxylic acid in good yield, and simple amidation provides **7**. Monomer **8** was synthesized in straightforward fashion (eq 4).



The syntheses of polymers **1**, **2**, **9**, and **10** were also accomplished by palladium-catalyzed coupling methodologies. The syntheses of polymer **3** and its accompanying model polymer **11** have been reported elsewhere.^{5b,c} The cross-



coupling method for polymer synthesis falls into the general category of a step-growth polymerization, wherein the molecular weight is related inversely to the extent of reaction.¹⁷ In a step-

(15) Zhou, Q.; Swager, T. M. *Polym. Prepr., Am. Chem. Soc. Div. Polym. Chem.* **1994**, 35 (1), 277–278.

(16) Similar results on bromide analogues have been reported previously: Lamba, J. J. S.; Tour, J. M. *J. Am. Chem. Soc.* **1994**, 116, 11723.

(17) Billmeyer, F. W. *Textbook of Polymer Science*; Wiley-Interscience: New York, 1984; Chapter 2.

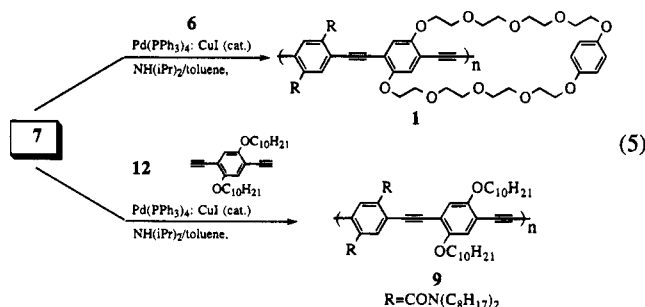
Table 1. Summary of Molecular Weight and Photophysical Data^a

polymer	GPC M_n	PDI	abs λ_{max} (nm) (ϵ)	emission λ_{max} (nm)	Φ	τ ($\times 10^{-9}$ s)	K_{SV} (M^{-1})
1	3.11×10^4	1.6	427 (3.9×10^4)	459	0.70	0.64	7.53×10^4
	6.54×10^4	1.6					1.01×10^5
	1.225×10^5	1.8					1.05×10^5
2	2.5×10^3	1.4	388 (4.4×10^4)	418	0.33	1.88	4.23×10^3
	1.6×10^4	2.8					1.06×10^4
3	6.5×10^3	2.0	520 (1.7×10^4)	624	0.066		5.34×10^3
4	$1.104^b \times 10^3$		367 (4.0×10^4)	401	0.77	1.18	1.63×10^3
9	2.688×10^5	2.9	428 (3.6×10^4)	459	0.76	0.66	5.74×10^2
	1.5×10^6	2.1					6.11×10^2
10	1.34×10^5	1.8	388 (3.5×10^4)	418	0.50	1.31	9.04×10^2
	2.53×10^5	1.7					1.42×10^3
11	1.19×10^4	1.9	534 (2.2×10^4)	622	0.058		
13	959 ^b		368 (6.6×10^4)	403	0.82	1.21	35.1

^a See Experimental Section for details of experimental conditions. ^b Determined by mass spectrometry.

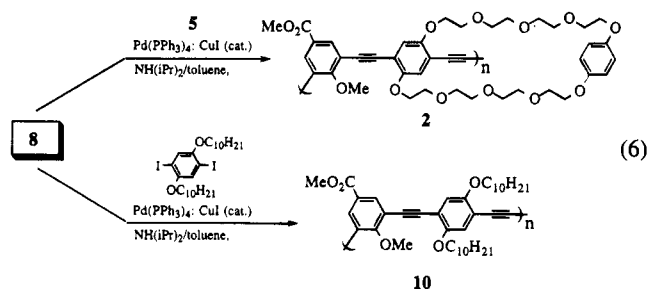
grow scheme, high molecular weight polymers are produced only if the yields of the coupling reactions are nearly quantitative. The molecular weights and PDIs for all of the polymers, along with other relevant physical data, are summarized in Table 1. In general, we found that the acetylene cross-coupling procedures used to produce **1**, **2**, **9**, and **10** can be effective for the syntheses of polymers with high molecular weights, indicating an essentially quantitative yield for these reactions. Key to producing polymers with very high molecular weights (i.e., $M_n \approx 100\,000$ or higher) was the use of a slight excess of the acetylene monomers (ca. 1.03 equiv). This adjustment is required to compensate for a very minor, yet seemingly unavoidable, competing side reaction, which involves oxidative coupling to produce diacetylene linkages. By varying the stoichiometry and reaction conditions, we produced a number of materials with different molecular weights (Table 1). These polymers have varying amounts of diacetylene linkages; however, these groups produce no detectable photophysical differences.

Monomer **7** served as **6**'s complement for the synthesis of polymer **1** (eq 5). Additionally, matching **7** with **12** produced polymer **9** (eq 5), which has the same electronic structure as **1** but lacks the cyclophane receptor. The choice of monomer **7**



was due to the fact that the electron-withdrawing amides provide high reactivity with the Pd⁰ catalysts. We have also found the dialkylamide group to provide excellent solubility for high molecular weight rigid-rod polymers. In our initial investigations, we synthesized polymer **1** by a functionalization scheme that was the reverse of that shown in eq 5. That is, we coupled the diiodocyclophane **5** with 2,5-diethynyl-1,4-bis(*N,N*-dioctylcarbamoyl)benzene to produce samples of **1** that are spectroscopically identical to **1** produced by eq 5. However, 2,5-diethynyl-1,4-bis(*N,N*-dioctylcarbamoyl)benzene is relatively unstable, and even with immediate purification prior to the polymerizations, we were not able to obtain molecular weights higher than 31 100. Polymers **2** and **10** were produced similarly (eq 6). The increased conformation entropy in these materials introduced by the meta linkages affords greater solubility, and

it was not necessary to introduce additional side chains. Polymers **1**, **9**, and **10** are prepared as soluble high molecular weight samples. In the case of **9**, we were able to prepare



ultrahigh molecular weight materials, with GPC molecular weights of 1.5×10^6 .¹⁸ We have found that the cyclophane-containing polymers **1** and **3** exhibit greater solubility than their nonmacrocyclic homologues **9** and **11**. However, we found that in the synthesis of polymer **2**, a sizable fraction of insoluble materials is produced. Hence, it appears that the cyclophane group in **2** produces specific associations or cross-links, possibly via catenane formation, which render it partially insoluble.

Photophysical Studies. The absorption and emission spectra of polymers **1–3** are shown in Figure 1. For all of the compounds studied, the excitation spectra were in agreement with the absorption spectra. Polymers **1**, **2**, **9**, and **10** are very highly emissive compounds and exhibit quantum yields ranging from 0.33 to 0.77 (Table 1). The polythiophenes are noticeably less emissive, with quantum yields of 0.066 and 0.058 for **3** and **11**, respectively. It is generally found that a conducting polymer's band gap is determined at very low degrees of polymerization. Consistent with this fact, all the absorption and emission spectra for the materials investigated were insensitive to molecular weight. The meta bridged systems, **2** and **10**, exhibited longer lifetimes and lower quantum yields than the para homologues, **1** and **9**, indicating a decreased radiative rate.

To determine the effect of the receptor on the quenching properties, we conducted parallel studies on polymers with the same electronic structures but lacking the cyclophane groups. It is necessary to ascertain the photophysical consequences (if any) resulting from the presence of cyclophane receptors in the polymers. Cyclophanes have been shown to be prone to intramolecular exciplex formation.¹⁹ Additionally, the large structural differences of cyclophane groups relative to simple alkyl side chains have the potential to influence the polymer's conformation. In polymers **1** and **9**, the backbone exhibits a

(18) The GPC method is known to overestimate the molecular weights of rigid-rod polymers. For a comparison of GPC and absolute M_n in a related system, see: Tour, J. M. *Trends Polym. Sci.* 1994, 2, 332.

(19) Diederich, F. *Cyclophanes*; Royal Society of Chemistry: London, 1991; pp 7–15 and references therein.

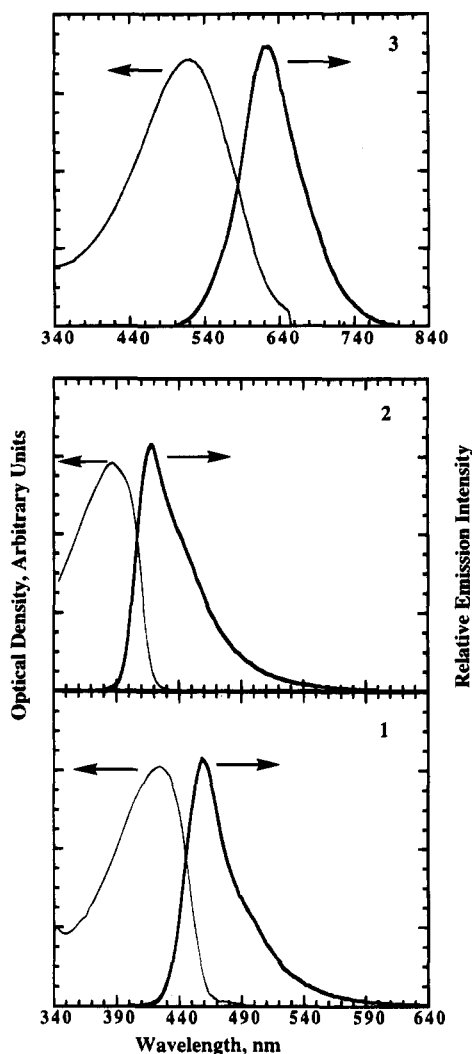


Figure 1. Absorption and emission spectra for 1–3 (details are given in the Experimental Section).

rigid-rod structure and is therefore immune to significant conformational changes. It follows, then, that the UV–vis and emission spectra of 1 and 9, with the exception of extra low wavelength absorptions assignable to the additional cyclophane phenyl, are identical. As a result, it appears that the cyclophane groups do not produce significant changes in the polymer's photophysical properties. Likewise, for polymers 2 and 10, which exhibit the potential for conformational isomerization, the observed absorption and emission characteristics are also extremely similar (Table 1). Polymer 3 displays absorption characteristics slightly different from those of its nonmacrocyclic homologue, 11 (Table 1). This difference likely originates from the fact that the bithiophene linkage is incorporated directly in the macrocycle, which restricts the polymer's conformation. This structure results in an absorption band for 11 that is 14 nm red-shifted from that of 3. Interestingly, the emission maximum is essentially the same for both 3 and 11, indicating that the excitations migrate to planarized segments of the polymer.

Figure 2 shows a side-by-side comparison of quenching results for 1 and the monomeric receptor 4. In the quenching studies, the macrocycle concentrations were held constant at 3.69×10^{-6} M, thereby ensuring the best comparison. The enhanced fluorescence quenching in the polymeric systems relative to the monomeric analogues is evident from simple inspection of the emission spectra as a function of PQ^{2+} . For example, at PQ^{2+} concentrations of 3.45×10^{-4} M, 4's emission is only diminished by about 30%, whereas 1's emission has

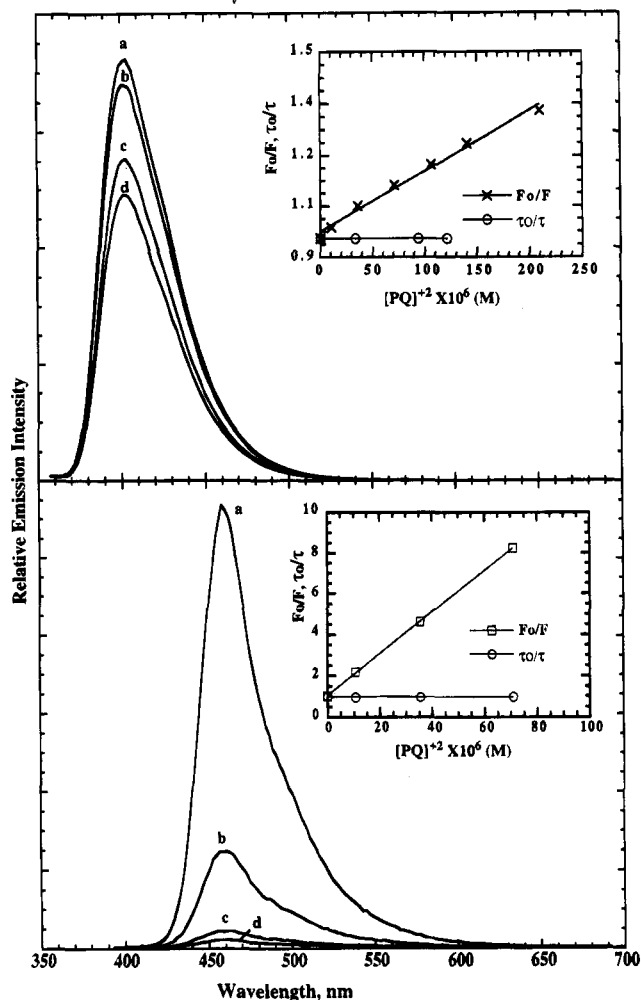


Figure 2. Emission spectra of 4 (top) and 1 (bottom) as a function of added PQ^{2+} . The curves are labeled to indicate the amount of PQ^{2+} added. For curve a, $[PQ^{2+}] = 0$; b, $[PQ^{2+}] = 3.56 \times 10^{-5}$ M; c, $[PQ^{2+}] = 2.10 \times 10^{-4}$ M; d, $[PQ^{2+}] = 3.45 \times 10^{-4}$ M. The Stern–Volmer plots are shown as insets, and the plots show τ_0/τ to be invariant with added PQ^{2+} .

been dramatically reduced to near background levels. As shown in Figures 3 and 4, both 2 and 3 also show a greater decrease in emission for a given PQ^{2+} concentration relative to 4.

To determine the differences between materials in a quantitative fashion, we have made use of the Stern–Volmer relationship,^{20,21}

$$F_0/F = 1 + K_{sv}[Q]$$

In this equation, F_0 is the fluorescence intensity without added quencher, F is the fluorescence intensity with added quencher, $[Q]$ is the quencher concentration, and K_{sv} is the Stern–Volmer constant. Quenching processes can be broadly characterized as being either static or dynamic in nature.²¹ Static processes are the result of quenching by a bound complex, which is the case for PQ^{2+} -occupied receptor sites. In the case of purely static quenching, K_{sv} is equal to the association constant, K_a .^{21,22} For static quenching, the diffusion rate of the quencher is not a factor, and the fluorescence lifetime is independent of $[Q]$. For purely dynamic quenching, the excited state is quenched by a

(20) Turro, N. J. *Modern Molecular Photochemistry*; Benjamin Cummings: Menlo Park, NJ, 1978.

(21) Lakowicz, J. R. *Principles of Fluorescence Spectroscopy*; Plenum Press: New York, 1986.

(22) Connors, K. A. *Binding Constants: The Measurement of Molecular Complex Stability*; Wiley-Interscience: New York, 1987.

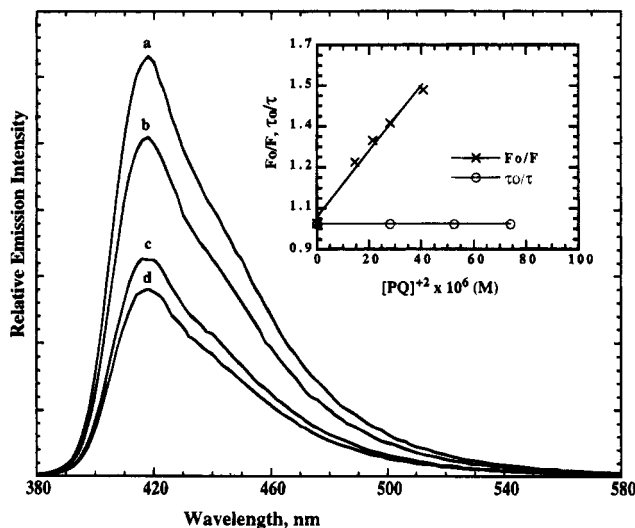


Figure 3. Emission spectra of **2** as a function of added PQ^{2+} . For curve a, $[PQ^{2+}] = 0$; b, $[PQ^{2+}] = 1.45 \times 10^{-5}$ M; c, $[PQ^{2+}] = 8.4 \times 10^{-5}$ M; d, $[PQ^{2+}] = 1.18 \times 10^{-4}$ M. The Stern–Volmer plot is shown as an inset, and τ_0/τ is shown to be invariant with added PQ^{2+} .

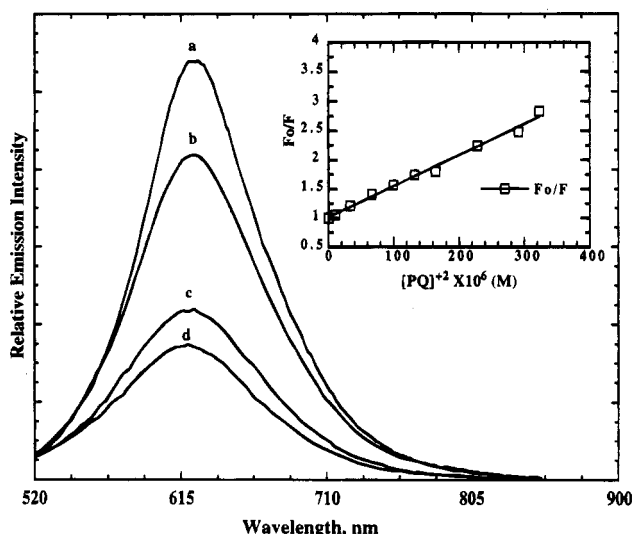


Figure 4. Emission spectra of **3** as a function of added PQ^{2+} . For curve a, $[PQ^{2+}] = 0$; b, $[PQ^{2+}] = 3.3 \times 10^{-5}$ M; c, $[PQ^{2+}] = 2.28 \times 10^{-4}$ M; d, $[PQ^{2+}] = 3.23 \times 10^{-4}$ M. The Stern–Volmer plot is shown as an inset.

collision with Q, and hence the lifetime is reduced with added quencher. A linear Stern–Volmer relationship will be observed if either static or dynamic quenching is dominant. Situations in which the two process are competitive give rise to nonlinear Stern–Volmer data.²¹

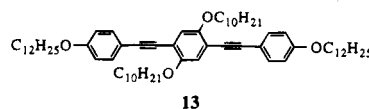
As shown in the insets of Figures 2–4, **1–4** all display linear Stern–Volmer relationships with added PQ^{2+} . The results of all the materials displaying such linear behaviors are summarized in Table 1. Additionally, measurements of the lifetime (τ) as a function of concentration, shown in the insets, for **1**, **2**, and **4** show no apparent changes. Hence, as expected, a static quenching process is dominant in these materials. Static quenching is also in accord with the host–guest complexation, which produces visibly detectable charge transfer absorptions. Dominant static quenching does not mean that diffusional quenching is not present, but rather that the quenching due to dynamic processes is negligible. In the case of **4**, the Stern–Volmer data reveal an association constant in acetone for the pseudorotaxane complex of 1630 M^{-1} , which is a little more than twice that determined for bis(*p*-phenylene-34-crown-10).¹³

The greater binding constant of **4** is a result of enhanced charge transfer interactions from the electron-donating nature of the *p*-(alkoxy)phenylacetylene groups and the extension of the unsaturated framework. Additionally, the greater preorganization that accompanies the added rigid *p*-(alkoxy)phenylacetylene groups also enhances binding. The binding constant of the simple bithiophene containing cyclophane has been determined by other methods^{5c} to be 1360 M^{-1} . As a result, we expect that the PQ^{2+} binding in polymer **3** (per receptor) will be roughly comparable to that observed for **1** and **2**.

As shown in Table 1, the Stern–Volmer constants for **1–3** indicate that these molecular wire-based materials exhibit quenching responses that are enhanced 2.6–65 times relative to that of the monomeric receptor **4**. Additionally, these measurements show polymer **1** to be more effective at energy migration than polymers **2** and **3**. The higher energy migration efficiency in **1** can be seen by considering that although **1** ($M_n = 31\,000$) has approximately twice the M_n of **2** ($M_n = 16\,000$), the K_{sv} for **1** is 7 times greater. This difference exists in spite of the fact that **1**'s lifetime is 0.64×10^{-9} s, which is about a factor of 3 shorter than that of **2** ($\tau = 1.88 \times 10^{-9}$ s). The fact that **2**'s excitations have longer lifetimes indicates that energy migration is slower in this system relative to **1**. While the exact molecular weights of **1** and **2** have not been determined, corrections would be too small to account for these differences.¹⁸ We have also considered other features that could invalidate our assessment that **1** displays a greater propensity for energy migration than **2**. One possibility is that the binding constants are lower in **2**. However, **2**'s cyclophane is substituted with phenylethynyl groups that bear electron-donating methoxy groups in the ortho positions. This structure should enhance binding of PQ^{2+} in **2** relative to **1**, which has electron-withdrawing *N,N*-diethylcarbamoyl groups. In addition **2**'s repeat formula weight is only 746, which is significantly smaller than that of **1** (1193), suggesting that, for a given molecular weight, **2** will have more receptor groups. This latter feature suggests that on a per receptor basis, energy migration is more efficient in **1** relative to **2** than the comparison of K_{sv} values would indicate. As a result, we conclude that **1** is clearly a superior structure for energy migration.

The greater tendency for energy migration for the all-para system **1** over **2** (with meta linkages) might be expected on the basis of delocalization. However, greater delocalization is not a guarantee of superior performance. This fact is illustrated by polymer **3**, which displays a K_{sv} roughly comparable to that of the lower molecular weight samples of **2** ($M_n = 2500$). This result indicates that **3** is less effective at energy migration than **1**, even though polythiophenes display much greater bandwidths (delocalization) relative to poly(phenyleneethylenes).

We have also studied quenching in the nonmacrocylic polymeric homologues **9–11**. Additionally, we have investigated **13**, which is a nonmacrocylic analogue of **4**. As men-



tioned earlier, these acyclic materials have photophysical properties that are extremely similar to those of the cyclophane-containing materials. Quenching studies on these materials also provide linear Stern–Volmer relationships. However, the K_{sv} constants (Table 1) are much lower than those of the cyclophane-containing materials. This latter fact is expected from purely dynamic quenching. The fluorescence lifetimes (τ) of **9**, **10**, and **13** were determined as a function of added PQ^{2+} ,

and a reduction in τ is observed with added PQ^{2+} , which is consistent with a dynamic quenching mechanism. The ratio of the lifetimes (τ_o/τ) can be used in place of the intensity ratios (F_o/F) to produce a Stern–Volmer plot. For constant radiative rates, plots of τ_o/τ vs $[\text{PQ}^{2+}]$ should yield Stern–Volmer plots with the same slope (K_{sv}). This analysis for **9** ($M_n = 268\,800$) yields $K_{sv}(\tau_o/\tau) = 400\text{ M}^{-1}$ ($K_{sv}(F_o/F) = 570\text{ M}^{-1}$), and for the meta-linked polymer, **10** ($M_n = 134\,000$), we obtain $K_{sv}(\tau_o/\tau) = 410\text{ M}^{-1}$ ($K_{sv}(F_o/F) = 904\text{ M}^{-1}$). We find particularly good agreement between the different K_{sv} determinations for the low molar mass analogue **13**, which yields $K_{sv}(\tau_o/\tau) = 32\text{ M}^{-1}$ and $K_{sv}(F_o/F) = 35\text{ M}^{-1}$. The differences between the lifetime (τ_o/τ) and fluorescence intensity (F_o/F) determinations of K_{sv} in **9** and **10** are not surprising, considering the polydisperse nature of these polymers. Additionally, polymer **10** likely exhibits a number of different conformations in solution, which may account for the bigger differences in the K_{sv} constants. Nevertheless, these determinations give K_{sv} constants of a similar magnitude and support our assertion that the quenching process in these systems is dynamic.

The receptorless polymers **9** and **11** also displayed enhancements in the K_{sv} relative to the model system, **13**. Depending upon M_n , samples of polymer **9** displayed a K_{sv} 16–18 times that displayed by **13**. This enhancement in K_{sv} is in spite of the fact that **9**'s lifetime (τ) is approximately half that displayed by **13**. Note that for dynamic quenching, K_{sv} is the product of τ and the diffusional rate constant. Additionally, the higher side chain density in **9** relative to **13** will impede diffusive quenching. Polymer **10** displayed even larger K_{sv} constants, which were a factor of 41 larger than that of **13** when $M_n = 253\,000$. Polymer **11** was not well-behaved in quenching studies, and the Stern–Volmer data were not linear. These results seem to indicate more complex interactions between PQ^{2+} and **11**. The enhancement in dynamic quenching due to energy migration in **9** and **10** arises from the increased effective dimension of the excited state. The increased area results in a greater probability for diffusional quenching by PQ^{2+} . The greater K_{sv} constants in the meta system (**10**) relative to the para material (**9**) are at first glance surprising, considering the greater static quenching observed for **1** relative to **2**. We believe that this result is due not to better energy migration but to other factors. One factor is the presence of bulky side chains in **9**, which makes quenching more difficult relative to **10**. Additionally, polymer **10**'s lifetime is about twice as long as that of **9**.

We have also probed the molecular weight dependence of the quenching process in polymers **1**, **2**, **9**, and **10**. In polymer **1**, we found K_{sv} to increase substantially when M_n is doubled from 31 000 to 65 000. However, when M_n is increased again from 65 000 to 122 000, the increase in K_{sv} is nearly undetectable. We found similar results in the other polymers. For **2**, K_{sv} increases significantly from 4.23×10^3 to $1.06 \times 10^4\text{ M}^{-1}$ when M_n is increased from 2500 to 16 000, respectively. Polymers **10** and **11** have only been investigated in high M_n form, wherein only slight increases in K_{sv} were observed with increasing molecular weight. These results are also explained in the context of energy migration. In the lower molecular weight samples, the diffusion length of the excitation exceeds the size of the molecule, and K_{sv} is limited by M_n . With high molecular weight materials, the diffusion length of the excitation, which is determined by the excited state lifetime and the excitation's diffusion rate, is limiting.

Summary and Outlook. We have demonstrated that systems in which a conjugated polymer (molecular wire) is used to interconnect (wire in series) receptor units lead to greatly enhanced fluorescence-based chemosensory responses relative

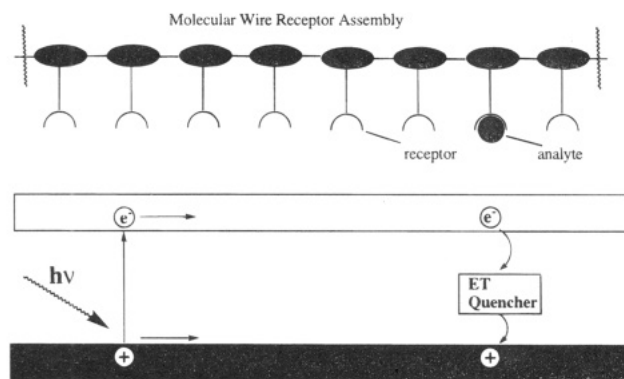


Figure 5. Schematic band diagram illustrating the mechanism by which the molecular wire receptor assembly can produce an enhancement in a fluorescence chemosensory response. The horizontal dimension represents the position along the conjugated polymer shown schematically at the top. Excitations are created by absorption of a photon ($h\nu$) and then migrate along the polymer backbone. Analyte binding produces a trapping site, whereby the excitation is effectively deactivated by electron transfer quenching.

to single receptor sensory molecules. The origin of this effect is the facile energy migration throughout the polymer. A key feature is that the energy migration is a property of the collective system rather than a property of discrete units of the polymer. A general schematic band diagram representation of the molecular wire enhancement methodology is shown in Figure 5. Although the pseudorotaxane formation involves the formation of charge transfer complexes, the electron transfer quenching mechanism need not involve direct intermolecular interactions with the analyte. Hence, this mechanism affords considerable design flexibility. Analyte binding events that introduce local narrowing of the band structure may also be used to produce amplified responses.²³ We are pursuing sensors based on this latter principle with recently developed methodologies, whereby conjugated polymer conformations are controlled with recognition events.^{5a}

We have made qualitative conclusions about the influence of the electronic structure on the ability of a material to display energy migration. The best comparisons can be made for polymers **1** and **2**. The meta substitution results in a less efficient energy migration, and a decreased mobility of the excitations in **2** can be inferred from its longer lifetimes. The less efficient energy migration was expected, considering the fact that decreased delocalization results in much lower conductivity in meta-linked polyphenylenes relative to para-linked materials.²⁴ However, the lower enhancements in the polythiophenes indicate that high delocalization, in and of itself, is not the sole determinant of the ability of a material to display efficient energy migration.

We have not determined the exact nature of the excitations in the materials studied. Determination of the character of the excitations will require additional investigations. However, based on other studies on poly(phenylenevinylenes) and polydiacetylenes,¹¹ we speculate that the low-polarizability nature of polymers **1** and **2** may favor excitons, whereas the more polarizable structure of **3** may favor free carriers. Clearly, the nature of the excitations will be a consideration in future optimization.

All of the studies reported herein were for isolated molecules in dilute solution. Many sensory applications will require the

(23) We have recently observed this phenomenon in a different system: Goldfinger, M. B.; Swager, T. M. *J. Am. Chem. Soc.* **1994**, *116*, 7895.

(24) Elsenbaumer, R. L.; Shacklette, L. W. In ref 2, Chapter 7, pp 213–263.

use of thin films coated on optical fibers. Qualitative studies on thin films of **1** have shown dramatic and reversible fluorescence quenching upon exposure to PQ^{2+} in H_2O/ACN solutions. The influence of the solid state organization (conformations) of the polymers will likely also play a role in determining the efficiency of energy migration.

Experimental Section

General. All chemicals were of reagent grade. Diisopropylamine was predried over NaOH and vacuum distilled. Anhydrous toluene and THF were purchased from Aldrich Chemical Co. Inc. All other solvents were used without further purifications. 1,4-Diiodo-2,5-dimethoxybenzene,²⁵ **12**,⁸ 1,4-bis(decyloxy)-2,5-diiodobenzene,⁸ and *p*-(dodecyloxy)phenylacetylene²³ were synthesized according to the literature procedures. NMR spectra were recorded on 250 or 200 MHz spectrometers, and chemical shifts were reported in ppm using $CHCl_3$, C_2HD_5SO , or C_2HD_5CO as internal reference. Mass spectroscopy was performed using $CHCl_3$ as solvent, and FAB spectra were measured in a 3-nitrobenzyl alcohol matrix. The molecular weights of polymers were determined by using Waters Ultrastaygel columns with 10^5 , 10^3 , and 500 Å pore sizes, a Rainin HPLC solvent delivery system, and a Dynamax refractive index detector, Model RI-1, at a flow rate of 1.0 mL/min in THF. All samples analyzed by GPC gave monomodal distributions. The molecular weights were reported relative to polystyrene standards purchased from Polysciences, Inc. Flash column chromatography was performed on 40 μm silica gel (Baker).

Photophysical Studies. Absorption and emission spectra of **1**, **3**, **4**, and **11** were obtained in acetone, those of **9** and **13** were obtained in acetone/THF (3:1), and those of **2** and **10** were obtained in acetone/THF (1:2). For all the materials, the measured excitation spectra were in agreement with the absorption spectra. The solvents were determined to be free of emitting impurities prior to use. In all quenching studies, care was taken to avoid changing the concentrations of the emitting compounds. This was accomplished by preparing the quencher in the same solutions of the emitting compounds. All emitting sample solutions were optically dilute at a concentration of 3.69×10^{-6} M (of repeat unit if the sample is polymer). Paraquat solutions used in the quenching studies of **1**, **3**, **4**, and **11** were prepared from respective solutions of **1**, **3**, **4**, and **11** at a concentration of 1.0×10^{-2} M; similar solutions were prepared for **2**, **9**, **10**, and **13** at a concentration of 9.66×10^{-4} M. The relative emission intensity for the Stern–Volmer analysis was recorded at the λ_{max} of the emission spectra. The samples were equilibrated after each addition of PQ^{2+} for 5 min with stirring prior to data collection. The UV–vis spectra were obtained from a Hewlett-Packard 8452A diode array spectrophotometer. Fluorescence studies were conducted with a Photon Technology International (PTI) M-III fluorometer. The spectra presented are uncorrected for the detector response and were performed in four-sided quartz cells at room temperature. For quantum yield measurements, an excitation wavelength of 346 nm was used, and quinine sulfate monohydrate (Aldrich) was employed as a standard (quantum yield of 0.55 in 1 N H_2SO_4). The quantum yield measurements for **1**, **4**, **9**, **10**, and **13** were performed in $CHCl_3$, that for **2** was performed in acetone, and those for **3** and **11** were performed in THF. Corrected fluorescence spectra were used for the quantum yield measurements, and the areas under the fluorescence spectra were obtained by integration at 2 nm intervals. The fluorescence lifetime measurements were performed as previously described,²⁶ and the reported values represent a best fit to a single exponential decay.

1,4-Diiodo-2,5-hydroquinone. 2,5-Diiodo-1,4-dimethoxybenzene (4.64 g, 11.9 mmol) was dissolved in CH_2Cl_2 (100 mL) in a 250 mL round-bottom flask fitted with a condenser. The reaction mixture was cooled to -80 °C in a dry ice–acetone bath. BBr_3 (23.8 mL, 1 M in CH_2Cl_2 , 23.8 mmol) was added slowly through the condenser. After the addition, a drying tube was attached on the top of the condenser, and the mixture was allowed to warm to room temperature. The mixture was stirred at room temperature for 48 h and then carefully hydrolyzed with H_2O (120 mL). The aqueous layer was separated and

extracted with ether (5×50 mL). The combined organic phases were extracted with NaOH (200 mL, 2 N), and then the NaOH solution was neutralized with dilute HCl in ice bath. The pink precipitate was collected and dried. Recrystallization from benzene gave light brown crystals (3.62 g, 84%, mp 195 – 197 °C): 1H NMR (250 MHz, acetone- d_6) 7.27 (s, 2H), 8.98 (s, 2H) ppm; ^{13}C (62.5 MHz, acetone- d_6) 84.41, 124.65, 151.54 ppm; IR (KBr) 3500, 3220, 3050, 2950, 2889, 1397, 1213, 755, 670 cm^{-1} ; MS m/z (relative intensity) 362 (M^+ , 100), 236, 210, 193, 183, 134.

1,4-Bis[2-(2-hydroxyethoxy)ethoxy]-2,5-diiodobenzene. This compound was prepared by an adaptation of the procedure for the preparation of 1,4-bis[2-(2-hydroxyethoxy)ethoxy]benzene^{13c} (70%, mp 104 – 105.5 °C): 1H NMR (250 MHz, $CDCl_3$) 1.81 (br s, 2 H), 3.67–3.71 (t, $J = 4.60$ Hz, 4 H), 3.74–3.77 (t, $J = 4.58$ Hz, 4H), 3.85–3.89 (m, 4H), 4.08–4.12 (m, 4H), 7.22 (s, 2H) ppm; ^{13}C NMR (62.5 MHz, $CDCl_3$) 61.73, 69.36, 69.97, 72.59, 86.38, 123.25, 152.90 ppm; IR (KBr) 3600, 3550, 3014, 2929, 2872, 1482, 1454, 1347, 1213, 1131, 1067, 929, 759 cm^{-1} ; MS m/z (relative intensity) 561 ($M^+ + Na$, 100), 538 (M^+), 450, 412, 362, 236, 176, 136, 107; HRMS calcd for $C_{14}H_{20}O_6I_2Na$ ($M^+ + Na$) 560.9247, found 560.9229.

Compound 5. This compound was prepared from 1,4-bis[2-(2-hydroxyethoxy)ethoxy]-2,5-diiodobenzene and 1,4-bis[2-(2-hydroxyethoxy)ethoxy]benzene ditosylate by adaptation of the procedure for the preparation of bis(*p*-phenylene-34-crown-10)^{13c} (14%, mp 105 – 107 °C): 1H NMR (250 MHz, $CDCl_3$) 3.68–3.86 (m, 24H), 3.94–4.02 (m, 8H), 6.71 (s, 4H), 7.15 (s, 2H) ppm; ^{13}C NMR (62.5 MHz, $CDCl_3$) 68.15, 69.50, 69.71, 70.29, 70.78, 70.88, 71.06, 86.38, 115.49, 123.29, 152.93, 153.01 ppm; MS m/z (relative intensity) 811 ($M^+ + Na$, 100), 788 (M^+), 662; HRMS calcd for $C_{28}H_{38}O_{10}I_2Na$ ($M^+ + Na$) 811.0452, found 811.0446. Anal. Calcd for $C_{28}H_{38}O_{10}I_2$: C, 42.64; H, 4.86. Found: C, 43.10; H, 4.97.

Compound 6. This compound was prepared according to a procedure similar to that which we reported for the preparation of 1,2-dialkyl-4,5-diethynylbenzene.²⁷ Disilane-protected intermediate was first obtained (80%, light yellow oil): 1H NMR (250 MHz, $CDCl_3$) 0.20 (s, 18 H), 3.55–4.03 (m, 32 H), 6.68 (s, 4 H), 6.85 (s, 2 H) ppm; ^{13}C NMR (62.5 MHz, $CDCl_3$) -0.16 , 67.93, 69.43, 69.59, 70.60, 70.69, 70.83, 70.98, 100.29, 100.77, 113.91, 115.32, 117.26, 152.82, 153.69 ppm. After deprotection, **6** is obtained in 90% yield as a pale white solid (mp 75.0 – 76.5 °C): 1H NMR (250 MHz, $CDCl_3$) 3.34 (s, 2 H), 3.53–4.08 (m, 32 H), 6.73 (s, 4 H), 6.90 (s, 2 H) ppm; ^{13}C NMR (62.5 MHz, $CDCl_3$) 68.02, 69.41, 69.50, 69.62, 70.68, 70.88, 79.39, 83.14, 113.46, 115.44, 118.08, 152.89, 153.93 ppm; IR (KBr) 3298, 3014, 2929, 2872, 2195, 1510, 1453, 1397, 1216, 1131, 769, 748, 663 cm^{-1} ; MS m/z (relative intensity) 602 ($M^+ + NH_3$), 584 (M^+), 313, 279 (100), 240, 203; HRMS calcd for $C_{32}H_{40}O_{10}N$ ($M^+ + NH_3$) 602.2965, found 602.2960. Anal. Calcd for $C_{32}H_{40}O_{10}$: C, 65.72; H, 6.90. Found: C, 65.82; H, 7.09.

2,5-Diiodo-*p*-xylene. This compound was synthesized according to the same procedure used for the preparation of 1,4-diiodo-2,5-dimethoxybenzene,²⁵ with the exception that the ratio of the solution was changed (for 0.15 mol of starting material, acetic acid/ H_2SO_4/H_2O , 500 mL/15 mL/50 mL). The compound was obtained as white crystals (84.5%, mp 104 – 105 °C [lit.⁴ mp 103 – 104 °C]): 1H NMR (250 MHz, $CDCl_3$) 2.32 (s, 6H), 7.62 (s, 2H) ppm; MS m/z (relative intensity) 358 (M^+), 231, 127, 104 (100).

4-Methyl-2,5-diiodobenzoic Acid. 1,4-Diiodo-*p*-xylene (15 g, 0.0419 mol) and $KMnO_4$ (40 g, 0.253 mol) were dissolved in the mixture of pyridine (150 mL, fresh distilled from $KMnO_4$) and H_2O (50 mL). The mixture was refluxed for 6 h and then filtered while it was still hot. The brown MnO_2 solid was rinsed with a hot 5% KOH solution, and the filtrate was dried *in vacuo*. The residue was then redissolved in water, filtered, cooled, and acidified with HCl in an ice–water bath. The white solid was collected and recrystallized from acetone/ H_2O to give white crystals (60%, mp 185 – 187 °C dec): 1H NMR (250 MHz, acetone- d_6) 2.42 (s, 3H), 7.98 (s, 1H), 8.27 (s, 1H) ppm; ^{13}C NMR (62.5 MHz, DMSO- d_6) 26.51, 93.93, 100.22, 135.17, 139.45, 141.07, 145.89, 165.85 ppm; MS m/z (relative intensity) 388 (M^+ , 100), 371, 254, 216, 127, 106.

2,5-Diiodo-1,4-dibenzoic Acid. To a mixture of 4-methyl-2,5-diiodobenzoic acid (10 g, 0.026 mol) in 10% KOH (100 mL) was added

(25) Jones, B.; Richardson, E. N. *J. Chem. Soc.* **1953**, 713.

(26) Holtom, G. R. *Proc. SPIE-Int. Soc. Opt. Eng.* **1990**, 1204, 1.

(27) Zhou, Q.; Carroll, P.; Swager, T. M. *J. Org. Chem.* **1994**, 59, 1294.

KMnO₄ (16.3 g, 0.104 mol) in one portion. The mixture was stirred and refluxed for 4 h. The hot mixture was filtered, and the brown solid MnO₂ was rinsed with hot 5% KOH solution. The filtrate was evaporated to half of its original volume *in vacuo* and then was acidified with 18% HCl. A light pink solid was collected and recrystallized from acetone/H₂O to give white needle crystals (85%, mp 235 °C dec): ¹H NMR (250 MHz, acetone-*d*₆) 4.30 (br s, 2H), 8.37 (s, 2H) ppm; ¹³C NMR (62.5 MHz, DMSO-*d*₆) 92.99, 140.02, 140.66, 165.94 ppm; MS *m/z* (relative intensity) 418 (M⁺, 100), 401, 374, 293, 275, 249.

2,5-Diiodo-1,4-dibenzoyl Chloride. 2,5-Diiodo-1,4-dibenzoic acid (15.4 g, 0.0368 mol) and thionyl chloride (30 mL) were combined and refluxed for 4 h, after which no more HCl gas was evolved. The excess SOCl₂ was removed *in vacuo*, and the residue was dissolved in hot hexane. The hot, clear hexane solution was decanted into another flask and cooled, whereupon light yellow crystals were obtained (86%, mp 195–197 °C): ¹H NMR (250 MHz, CDCl₃) 8.41 (s, 2H) ppm; ¹³C NMR (62.5 MHz, CDCl₃) 91.28, 143.17, 143.35, 165.20 ppm; MS *m/z* (relative intensity) 454 (M⁺), 419 (100), 391, 371, 356, 293, 229, 201, 127.

1,4-Bis(*N,N*-dioctylcarbamoyl)-2,5-diiodobenzene (7). 2,5-Diiodo-1,4-dibenzoyl chloride (1.4 g, 3.08 mmol) and dioctylamine (3.2 g, 13.24 mmol) were dissolved in CH₂Cl₂ (50 mL), and this mixture was refluxed for 7 h. The reaction mixture was cooled and washed with 10% HCl, H₂O, and brine. The organic phase was dried over MgSO₄, and the solvent was removed *in vacuo*. Chromatography (CH₂Cl₂/acetone 10:1) of the residue gave a colorless oil which became a waxlike solid after being stirred under high vacuum for 5 h (80%, mp 53–55 °C): ¹H NMR (250 MHz, CDCl₃) 0.85 (m, 12H), 1.05–1.7 (m, 48H), 2.9–3.2 (m, 6H), 3.67 (m, 2H), 7.55 (s, 2H) ppm; ¹³C NMR (62.5 MHz, CDCl₃) 14.07, 22.60, 26.65, 26.95, 27.19, 28.42, 29.10, 29.24, 29.33, 31.66, 31.79, 44.54, 48.53, 92.41, 137.37, 144.28, 168.28 ppm; MS *m/z* (relative intensity) 887 (M⁺ + Na), 865 (M⁺ + H, 100), 737, 624, 498, 401; HRMS calcd for C₄₀H₇₁O₂I₂ (M⁺ + H) 865.3605; found 865.3619. Anal. Calcd for C₄₀H₇₀O₂I₂: C, 55.53; H, 8.16. Found: C, 55.09; H, 8.19.

2,5-Diethynyl-1,4-bis(*N,N*-dioctylcarbamoyl)benzene. To a mixture of 7 (1.50 g, 1.74 mmol), Pd(PPh₃)₂Cl₂ (0.025 g, 0.035 mmol), and CuI (0.010 g, 0.050 mmol) in diisopropylamine (30 mL) under an atmosphere of argon was added (trimethylsilyl)acetylene (0.54 mL, 3.83 mmol) dropwise, and then the mixture was heated at 70 °C overnight. The mixture was dried *in vacuo*, and the residue was chromatographed (hexane/CH₂Cl₂/ethyl acetate 20:5:1) to yield a light yellow oil (1.26 g, 90%): ¹H NMR (250 MHz, CDCl₃) 0.16 (s, 18H), 0.84 (t, *J* = 5.0 Hz, 12H), 1.0–1.7 (m, 48H), 3.05 (t, *J* = 5.2 MHz, 4H), 3.2 (m, 2H), 3.55 (m, 2H), 7.30 (s, 2H) ppm; ¹³C NMR (62.5 MHz, CDCl₃) –0.38, 13.99, 22.52, 26.51, 27.07, 27.30, 28.50, 28.98, 29.14, 29.18, 29.27, 31.59, 31.72, 44.70, 48.65, 100.55, 101.02, 120.14, 130.55, 139.84, 168.05 ppm; MS *m/z* (relative intensity) 805 (M⁺, 100), 693, 564.

The compound prepared above was dissolved in a mixture of KOH (two tablets in 1 mL of H₂O) and MeOH (100 mL, degassed) and stirred at room temperature for 0.5 h. The mixture was subjected to a CHCl₃/H₂O workup. The organic phases were combined and dried over MgSO₄. The solvent was removed *in vacuo*, and the residue was chromatographed (CHCl₃/hexane/ethyl acetate 1:3:0.02) to afford a pale yellow solid (0.881 g, 85%, mp 49.0–50.5 °C): ¹H NMR (250 MHz, CDCl₃) 0.84 (t, *J* = 5.4 Hz, 12H), 1.0–1.7 (m, 48H), 3.06 (t, *J* = 7.3 Hz, 4H), 3.22 (s, 2H), 3.2–3.7 (m, 4H), 7.36 (s, 2H) ppm; ¹³C NMR (62.5 MHz, CDCl₃) 14.03, 22.59, 26.54, 27.07, 28.45, 29.06, 29.18, 29.24, 29.36, 31.63, 31.80, 44.36, 48.45, 79.85, 83.00, 119.76, 130.73, 140.49, 168.04 ppm.

Polymer 1 (*M*_n = 31 100). Under an atmosphere of argon, diisopropylamine/toluene (3:7, 2 mL) solvent was added to a 25 mL Schlenk flask containing 2,5-diethynyl-1,4-bis(*N,N*-dioctylcarbamoyl)benzene (0.120 g, 0.182 mmol), 5 (0.139 g, 0.177 mmol), CuI (10 mg, 0.053 mmol), and Pd(PPh₃)₄ (12.5 mg, 0.0108 mmol). This mixture was heated at 70 °C for 5 h and then subjected to a CHCl₃/H₂O workup. The combined organic phase was washed with NH₄OH (50%), H₂O, HCl solution (5%), saturated NaHCO₃, and H₂O and dried over MgSO₄. The solvent was removed *in vacuo*, and the residue was washed with MeOH until the solution was colorless. The polymer was a yellow solid (0.19 g, 85%): ¹H NMR (250 MHz, CDCl₃) 0.80–0.91 (m, 12H),

0.94–1.36 (m, 48H), 3.1 (br s, 4H), 3.25–4.1 (br m, 36H), 6.67 (br s, 4H), 6.85 (br s, 2H), 7.48 (br s, 2H) ppm; ¹³C NMR (62.5 MHz, CDCl₃) 13.55, 22.11, 22.18, 26.26, 26.74, 27.09, 28.25, 28.55, 28.68, 28.86, 29.16, 29.47, 29.78, 30.09, 30.39, 31.21, 31.34, 44.50, 48.77, 67.57, 69.07, 69.25, 70.18, 70.46, 91.01, 92.03, 113.61, 114.84, 116.95, 119.93, 129.83, 139.47, 152.52, 153.21, 167.70 ppm. Anal. Calcd for C₇₂H₁₀₈N₂O₁₂: C, 72.44; H, 9.13; N, 2.35. Found: C, 72.39; H, 9.36; N, 2.78. Polymer 1 (*M*_n = 65 400) was prepared according to the same procedure as above, except the starting monomers were 7/6 (1:1.02, 0.2256 mmol of 7) (90% yield). Polymer 1 (*M*_n = 122 000) was prepared according to the same procedure as above, except the starting monomers were 7/6 (1:1.02, 0.2256 mmol of 7) (95% yield).

Model Compound 4. Under an argon atmosphere, diisopropylamine (15 mL) was added to a mixture of 5 (0.084 g, 0.107 mmol), 4-(dodecyloxy)phenylacetylene (0.063 g, 0.2201 mmol), Pd(PPh₃)₄ (6 mg, 0.0054 mmol), and CuI (4 mg, 0.02 mmol). The mixture was heated at 75 °C for 6 h. The solvent was removed *in vacuo*, and the residue was column chromatographed (CHCl₃/hexane 1:3) to afford 4 as a pale yellow powder (0.097 g, 80%, mp 60 °C): ¹H NMR (250 MHz, CDCl₃) 0.83 (t, *J* = 6.96 Hz, 6H), 1.12–1.48 (m, 36H), 1.67–1.85 (m, 4H), 3.56–4.15 (m, 36H), 6.67 (s, 4H), 6.85 (d, *J* = 8.58 Hz, 4H), 6.95 (s, 2H), 7.45 (d, *J* = 8.69 Hz, 4H) ppm; ¹³C NMR (62.6 MHz, CDCl₃) 14.10, 22.67, 26.01, 29.19, 29.34, 29.58, 31.90, 68.06, 69.59, 69.70, 70.80, 70.91, 71.08, 84.53, 95.24, 114.09, 114.49, 115.19, 115.42, 116.89, 133.02, 152.93, 153.41, 159.28 ppm; IR (KBr) 3007, 2922, 2851, 2210, 1606, 1514, 1244, 1216, 1131, 758, 670 cm⁻¹; MS *m/z* (relative intensity) 1128 (M⁺ + Na), 1106 (M⁺ + H), 958, 635, 458, 401, 352 (100); HRMS calcd for C₆₈H₉₆O₁₂Na (M⁺ + Na) 1127.6800, found 1127.6815.

Polymer 9 (*M*_n = 269 000). This polymer was prepared according to the same procedure as the one used for polymer 1. The monomers were 7 and 1,4-didecoxy-2,5-diethynylbenzene (12) (1:1, 0.2281 mmol), and the reaction time was 5 h. The polymer is a bright yellow orange solid (90%): ¹H NMR (250 MHz, CDCl₃) 0.83 (m, 18H), 1.0–1.55 (m, 62H), 1.75 (br m, 4H), 3.05–3.25 (br m, 8H), 3.91 (br m, 4H), 6.86 (br s, 2H), 7.45 (br s, 2H) ppm; IR (KBr) 3021, 2922, 2851, 2212, 1627, 1648, 1230, 1202, 790, 727, 670 cm⁻¹. Anal. Calcd for C₇₀H₁₁₄N₂O₄: C, 80.24; H, 10.97; N, 2.68. Found: C, 80.18; H, 11.19; N, 2.67. Polymer 9 (*M*_n = 1.5 × 10⁶) was prepared according to the same procedure as above, except the monomer ratio was 1:1.03 (0.2281 mmol of 7), (98% yield).

Model Compound 13. This compound was prepared according to the same procedure as the one used for 4. The starting materials were 1,4-didecoxy-2,5-diethynylbenzene (0.1 g, 0.2281 mmol) and 1-dodecoxy-4-iodobenzene (0.195 g, 0.5018 mmol). 13 is a bright yellow powder (0.175 g, 80%, mp 62.5–64.5 °C): ¹H NMR (250 MHz, CDCl₃) 0.86 (m, 12H), 1.1–1.55 (m, 64H), 1.77 (m, 8H), 3.95 (t, *J* = 6.62 Hz, 4H), 3.40 (t, *J* = 6.49 Hz, 4H), 6.85 (d, *J* = 8.73 Hz, 4H), 6.97 (s, 2H), 7.45 (d, *J* = 8.67 Hz, 4H) ppm; ¹³C NMR (62.5 MHz, CDCl₃) 14.12, 22.69, 26.04, 26.10, 29.21, 29.38, 29.60, 31.92, 68.06, 69.65, 84.63, 94.88, 114.01, 114.47, 115.40, 116.87, 132.99, 153.49, 159.22 ppm; IR (KBr) 2922, 2851, 2212, 1606, 1514, 1471, 1244, 1174, 833, 759 cm⁻¹; MS *m/z* (relative intensity) 959 (M⁺, 100) 818, 679, 621, 490, 413, 329; HRMS calcd for C₆₆H₁₀₃O₄ (M⁺ + H) 959.7856, found 959.7840. Anal. Calcd for C₆₆H₁₀₂O₄: C, 82.60; H, 10.72. Found: C, 83.08; H, 11.09.

Methyl 4-Hydroxy-3,5-diiodobenzoate. To a solution of 4-hydroxy-3,5-diiodobenzoic acid (4 g, 0.01026 mol) in MeOH (200 mL) was added H₂SO₄ (concentrated 20 drops). The solution was refluxed overnight. The solvent was evaporated, and the residue was recrystallized twice from MeOH/H₂O to generate white needle crystals (3.8 g, 92%, mp 171.5–173 °C): ¹H NMR (250 MHz, CDCl₃) 3.87 (s, 3H), 6.05 (br s, 1H), 8.33 (s, 2H) ppm; ¹³C NMR (62.5 MHz, acetone-*d*₆) 52.42, 81.552, 117.05, 125.99, 140.84, 157.16 ppm; IR (KBr) 3468, 3014, 2957, 2929, 2858, 1713, 1283, 1262, 1220, 787, 702 cm⁻¹; MS *m/z* (relative intensity) 404 (M⁺, 100), 373, 245, 218, 189, 150 119. Anal. Calcd for C₈H₆O₃I₂: C, 23.77; H, 1.50. Found: C, 23.60; H, 1.50.

Methyl 4-Methoxy-3,5-diiodobenzoate: A mixture of methyl 4-hydroxy-3,5-diiodobenzoate (3.42 g, 8.47 mmol), potassium carbonate (10 g, 0.072 mol), and iodomethane (12.0 g, 0.0847 mol) in 120 mL of acetone (120 mL, predried by anhydrous K₂CO₃) was refluxed for

16 h. After being cooled to room temperature, the mixture was filtered, the solvent was evaporated, and the residue was recrystallized from MeOH to generate the product as white needle crystals (3.18 g, 90%, mp 91–93 °C): $^1\text{H NMR}$ (250 MHz, CDCl_3) 3.83 (s, 3H), 3.88 (s, 3H), 8.40 (s, 2H) ppm; $^{13}\text{C NMR}$ (62.5 MHz, acetone- d_6) 52.86, 61.06, 90.87, 130.17, 141.64, 163.51, 163.90 ppm; IR (KBr) 3021, 3007, 2950, 1723, 1440, 1411, 1276, 993, 769, 705 cm^{-1} ; MS m/z (relative intensity) 418 (M^+ , 100), 387, 276, 245; HRMS calcd for $\text{C}_9\text{H}_8\text{O}_3\text{I}_2$ (M^+) 417.8563, found 417.8568. Anal. Calcd for $\text{C}_9\text{H}_8\text{O}_3\text{I}_2$: C, 25.84; H, 1.93. Found: C, 26.03; H, 1.98.

Methyl 3,5-Diethynyl-4-methoxybenzoate (8). To a mixture of methyl 4-methoxy-3,5-diiodobenzoate (1.47 g, 3.52 mmol), $\text{Pd}(\text{PPh}_3)_2\text{Cl}_2$ (0.049 g, 0.07 mmol), and CuI (0.020 g, 0.105 mmol) in diisopropylamine (30 mL) was added (trimethylsilyl)acetylene (1.09 mL, 7.74 mmol) dropwise, and then the mixture was heated at 60 °C overnight. The mixture was dried *in vacuo*, and the residue was chromatographed (hexane/ CH_2Cl_2 /ethyl acetate 20:5:1) to yield a white solid (1.20 g, 3.34 mmol, mp 55–57 °C): $^1\text{H NMR}$ (250 MHz, CDCl_3) 0.24 (s, 18H), 3.87 (s, 3H), 4.11 (s, 3H), 8.02 (s, 2H) ppm; $^{13}\text{C NMR}$ (62.5 MHz, CDCl_3) -0.245, 52.24, 60.97, 99.73, 100.29, 116.82, 124.93, 135.58, 165.36, 167.07 ppm; IR (KBr) 3014, 2957, 2901, 2149, 1720, 1468, 1440, 1411, 1319, 1248, 1233, 1007, 844, 766 cm^{-1} ; MS m/z (relative intensity) 358 (M^+ , 100), 343, 327, 255, 164.

The above compound was dissolved in a mixture of KOH (two tablets in 1 mL of H_2O) and MeOH (100 mL, degassed) and stirred at room temperature for 1 h. The mixture was subjected to a $\text{CHCl}_3/\text{H}_2\text{O}$ workup. The organic phases were combined and dried over MgSO_4 . The solvent was removed *in vacuo*, and the residue was chromatographed (CHCl_3 /hexane/ethyl acetate 1:3:0.02) and recrystallized from MeOH to generate white fluffy crystals (0.69 g, 97%, mp 114.5–115.5 °C): $^1\text{H NMR}$ (250 MHz, CDCl_3) 3.31 (s, 2H), 3.86 (s, 3H), 4.12 (s, 3H), 8.07 (s, 2H) ppm; $^{13}\text{C NMR}$ (62.5 MHz, CDCl_3) 52.30, 61.41, 78.47, 82.70, 115.79, 125.11, 136.23, 165.07, 166.02 ppm; IR (KBr) 3298, 3021, 2950, 2362, 1723, 1443, 1315, 1223, 1202, 1003, 759, 666 cm^{-1} ; MS m/z (relative intensity) 214 (M^+ , 100), 183, 140, 127, 112; HRMS calcd for $\text{C}_{13}\text{H}_{10}\text{O}_3$ (M^+) 214.0629, found 214.0622. Anal. Calcd for $\text{C}_{13}\text{H}_{10}\text{O}_3$: C, 72.88; H, 4.71. Found: C, 73.20; H, 4.83.

Polymer 10 ($M_n = 253\ 000$). This polymer was prepared according to the same procedure as the one used for polymer 1. The monomers

were **8** and 1,4-bis(tetradecyloxy)-2,5-diiodobenzene (1.03:1.00, 0.4671 mmol of **8**), and the reaction time was 16 h. The polymer is a bright yellow solid (98%): $^1\text{H NMR}$ (250 MHz, CDCl_3) 0.84 (m, 6H), 1.0–1.55 (m, 40H), 1.81 (br m, 4H), 3.91 (br s, 3H), 4.03 (br t, 4H), 4.35 (br s, 3H), 7.02 (br s, 2H), 8.14 (br s, 2H) ppm; $^{13}\text{C NMR}$ (62.5 MHz, CDCl_3) 14.10, 22.68, 25.98, 29.35, 29.67, 31.91, 52.26, 61.46, 69.53, 90.26, 91.24, 113.85, 116.48, 116.76, 124.76, 135.37, 153.68, 163.88, 165.5 ppm. Anal. Calcd for $\text{C}_47\text{H}_{68}\text{O}_5$: C, 79.16; H, 9.62. Found: C, 78.55; H, 9.76. Polymer **13** ($M_n = 134\ 000$) was prepared according to the same procedure as above, except the monomer ratio was 1.00:1.01 (0.461 mmol of **8**) (98% yield).

Polymer 2 ($M_n = 16\ 000$). This polymer was prepared according to the same procedure as used the one for polymer 1. The monomers were **8** and **5** (1.03:1, 0.2335 mmol of **8**), and the reaction time was 16 h. The polymer is a yellow solid (10%; rest of the polymer does not dissolve in common organic solvents): $^1\text{H NMR}$ (250 MHz, CDCl_3) 3.55–3.9 (m, 28 H), 3.92 (br s, 3 H), 4.13 (br t, 4 H), 4.34 (br s, 3 H), 6.69 (br s, 4 H), 7.02 (br s, 2 H), 8.13 (br s, 2 H) ppm; $^{13}\text{C NMR}$ (50 MHz, CDCl_3) 29.66, 52.30, 61.67, 68.03, 69.36, 69.69, 70.64, 70.79, 70.88, 90.56, 91.12, 114.05, 115.36, 116.43, 117.03, 125.05, 135.39, 152.93, 153.68, 164.55, 165.40 ppm; IR (neat) 3014, 2929, 2872, 1720, 1507, 1479, 1450, 1351, 1230, 1216, 1131, 1060, 773, 744 cm^{-1} . Polymer **2** ($M_n = 2500$) was a mixture of oligomers, prepared according to the same procedure, except the reaction was done at room temperature for 16 h.

Acknowledgment. Funding to T.M.S. from the National Science Foundation MRL program (DMR-9120668), a NYI award (DMR-9258298), a DuPont Young Professor Grant, and an Alfred P. Sloan Fellowship is greatly appreciated. We also thank Dr. M. J. Marsella for providing samples of the polythiophenes used in this study. Lifetime measurements were performed at the National Institutes of Health Regional Laser and Biotechnology Laboratory at the University of Pennsylvania (NIH-RR-01348). We thank Dr. Luis Jahn for his assistance in obtaining the lifetime measurements.

JA953074X